Coupled CFD and building energy simulations for studying the impacts of building height topology and buoyancy on local urban microclimates

Jonas Allegrini [a,b*], Jan Carmeliet [a,b]

[a] Laboratory for Multiscale Studies in Building Physics
Swiss Federal Laboratories for Materials Science and Technology (Empa)
Überlandstrasse 129, 8600 Dübendorf, Switzerland

[b] Chair of Building Physics, Swiss Federal Institute of Technology Zurich (ETHZ),
Stefano-Franscini-Platz 1, 8093 Zürich, Switzerland

Abstract:

The temperatures in cities are increased due to the urban heat island effect. Heat can be removed from urban areas by wind and buoyancy driven ventilation. Building geometries have a strong impact on the wind flow patterns and heat removal in urban areas. The microclimate is analysed for a generic urban area with 23 buildings. Six different urban topologies are studied, where only the building heights of the individual buildings are changed. The local air temperatures are studied with coupled CFD and building energy simulations. The results show that the building height topology has a minimal impact on the mean air temperatures, but influences local air temperatures and the size of local heat islands. An analysis based on a comparison of simulations with / without buoyancy, shows a strong impact of buoyancy on the mean and local air temperatures. Further, correlations are found showing that the normalised increase in local air temperature is linked to the local air volume flow rates and thermal diffusivities. With higher volume flow rates and thermal diffusivities more heat can be removed from the environment. Based on these correlations an approach to evaluate the local heat island formation risk using isothermal CFD simulations is proposed.

Keywords

Urban Heat Island Effect, Computational Fluid Dynamics, Pedestrian Thermal Comfort, Microclimate, Urban Design, Buoyancy

Corresponding author: Jonas Allegrini, Empa Dübendorf, Ueberlandstrasse 129, 8600 Dübendorf, Switzerland. Tel.: +41 (0) 58 765 65 12, Fax: +41 (0) 58 765 40 09, e-mail: jonas.allegrini@empa.ch

1. Introduction

It is well known that the microclimate in urban areas differs significantly from the climate in rural areas. Air temperatures are higher due to the urban heat island effect and wind speeds are lower due to wind sheltering leading to decreased removal of heat and pollutants from urban areas (Oke 1987). Measurements in London showed up to 7 K higher air temperatures at night-time in the city com-

pared to measurements outside the city (Watkins et al. 2002). In Athens the mean heat island intensity exceeds 10 K (Santamouris et al. 2001). The urban microclimate influences strongly the energy demand for space cooling and heating of buildings, and it has also a large impact on the thermal comfort and health of the people living in urban areas. Global warming and associated heat waves (Schär et al. 2004, Fischer and Schär 2009) may further increase the temperatures in urban areas and can e.g. reduce the potential for night cooling significantly. Li and Bou-Zeid (2013) showed that the combined effect of UHI and heat waves is larger than the sum of the two individual effects. The UHI effect has a large impact on the thermal comfort (e.g. Saneinejad et al. 2014) and health (e.g. Robine et al. 2008) of pedestrians and on energy demand of buildings in urban areas (e.g. Allegrini et al. 2012a, Bouyer et al. 2011).

Knowledge of the detailed urban microclimate is important for a wide number of applications. A wide range of numerical studies on the microclimate can be found in literature. Arnfield (2003), Mirzaei and Haghighat (2010) and Moonen et al. (2012) give overviews over such microclimate studies. In the literature the local urban microclimate is numerically studied with different degrees of complexity and for different length scales, different numerical models are applied. Computational Fluid Dynamics (CFD) simulations are often used for microclimate simulations at the neighbourhood scale due to its high spatial resolution. For larger scales these simulations get computationally too expensive. As an example we mention recent microclimate studies based on CFD simulations e.g.by Toparlar et al. (2015), Gromke et al. (2015), Allegrini et al. (2015a) and Allegrini et al. (2015b).

Two types of microclimate or wind flow studies can be found in literature: studies with generic building configurations (a list of a number of studies is given in Ramponi et al. 2015) and studies for existing mostly complex building configurations (e.g. Toparlar et al. 2015, van Hooff and Blocken 2010). For most of the studies with generic building configurations, all buildings have the same building height and the influence of non-uniform building heights in an array of buildings is not analysed in detail (except flows around high-rise buildings).

A number of studies, where the impact of non-uniform building heights on the flow in urban areas is studied, can be found in literature. Tominaga (2012) conducted a CFD study, where he first analysed the ventilation efficiency in a generic urban area with non-uniform building heights, before he studied the ventilation for a real urban configuration. For the generic cases he kept the average building height constant. He found lower wind speeds and higher temperatures for building configurations with uniform (lower) building heights, compared to the cases with high-rise buildings surrounded by low-rise buildings. He reported that the high-rise buildings have a positive effect on the ventilation potential of an urban area. Also Hang et al. (2012) studied the influence of building height variability on ventilation in urban areas. They mainly focused on pollutant dispersion. As Tominaga (2012), they conducted their study with a generic building configuration with block-type buildings, which had variable building heights. The results of this study show improved ventilation for urban areas with non-uniform building heights. Boppana et al. (2010) conducted a similar study,

but used a staggered configuration of the building blocks instead of the configuration, where the buildings are aligned as it was used by Hang et al. (2012). They used LES (Large Eddy Simulations) to account for the unsteady flow structures and found that the ventilation is influenced by the higher turbulence intensities caused by the non-uniform building heights. Gan and Chen (2016) analysed the influence of different building height topologies on the wind flow patterns within the urban areas. They found a correlation between the rugosity of the urban area and the wind speed at the pedestrian level.

Besides studies that focus on the wind flow patterns and on pollutant dispersion also a number of studies have been conducted, where the influence of the building height topology on the air temperatures in an urban environment and the removal of heat was investigated. Pillai et al. (2010) and Pillai and Yoshie (2015) used CFD simulations to analyse the heat removal from generic urban areas with uniform and non-uniform building heights. The results showed increased heat transfer for cases with non-uniform building heights. They further used their results for urban canopy models in mesoscale meteorological models for better urban heat island predications. Deng et al. (2016) used ENVI-met (Bruse and Fleer 1998) to study the thermal comfort in urban areas dependent on the building height topology. They found a larger impact of the building height topology on the wind speed than on the air temperatures. Only average and not local air temperatures were reported. We note however that the local air temperature might vary significantly compared to the average one and also between different cases.

Finally also a number of studies have been conducted to analyse the influence of the building height topology on the larger scale flow phenomena. Studies were conducted, where the aerodynamic parameters (e.g. drag coefficients, roughness lengths, displacement heights) were determined for urban areas with uniform and non-uniform building heights. For example Zaki et al. (2011) and Millward-Hopkins et al. (2011) found an influence of the building height topology on the aerodynamic parameters (e.g. roughness lengths and displacement heights), of urban building arrays.

A large number of studies that investigate the ventilation of urban areas focus on pollutant dispersion and consider isothermal conditions. The results of these studies cannot directly be used to analyse the heat removal potential of urban areas. Heat is an active and not a passive scalar. Therefore buoyancy effects have to be considered. Buoyancy has a strong impact on the flow fields and the heat removal potential for weather conditions with high temperatures and calm winds, which are the most critical for thermal comfort. For example Allegrini et al. (2015a) showed that buoyancy has an impact on the local air temperatures in urban areas. Buoyancy increases urban ventilation and therefore decreases the local air temperatures. Allegrini et al. (2015a) conducted CFD simulations, which were coupled with building energy simulations (BES) including detailed shortwave and thermal radiation models to achieve accurate temperatures for the surface boundary conditions. Similar approaches have been used by Santiago et al. (2014), Yaghoobian et al. (2014), Nazarian and Kleissl (2015) and Nazarian and Kleissl (2016), who found an important impact of buoyancy on the vortex

structure between an array of cubical buildings. Besides flow field results also detailed results of surface temperatures and surface heat fluxes can be found in these publications.

For a better understanding of the formation of urban and local heat islands, it is important to understand the heat transfer in urban areas. Allegrini et al. (2015b) studied the heat fluxes in generic urban areas with different urban morphologies. They found that for high wind speed conditions, when the flow was in a forced convective flow regime, a large part of the heat is removed due to turbulence at the roof height. This means that not only convective but also turbulent heat fluxes have to be analysed to understand the heat flow in urban areas. The importance of accounting for the turbulent fluxes was also shown by Moonen et al. (2011) and Nazarian and Kleissl 2016. Moonen et al. (2011) compared air exchange rates only considering the convective fluxes using RANS (Reynolds-average Navier-Stokes) and large eddy simulations (LES). For the RANS simulations the time averaged flow field was used for the calculation, while the instantaneous flow field were used for the LES. The air exchange rates from the RANS simulations were considerably lower compared to the exchange rates of the LES, because only for the LES the air exchange due to turbulence was considered with the used analysis method. However, Allegrini et al. (2015a) also showed that for low wind speed conditions, that buoyancy improves heat removal with a shift of the heat removal mechanism from turbulence to convective flow.

The aim of this study is to analyse the impact of different building height topologies and buoyancy on the local microclimate in an urban environment. For this study the same numerical approach as in Allegrini et al. (2015a) and Allegrini et al. (2015b) is used. Building surface temperatures are determined with BES and then used in RANS (Reynolds-Averaged Navier-Stokes) CFD simulations as boundary conditions (one-way coupling). Compared to the two previous studies, here only one urban morphology is used, namely an array of staggered block-type buildings. In this study, the heights of the individual buildings are changed for the different cases, while uniform building heights were used in the two previous studies (Allegrini et al. 2015a and Allegrini et al. 2015b). Special focus is on the impact of buoyancy on the heat removal potential of an urban area. Simulations for mixed and forced convective conditions are conducted to study the performance of the different building height topologies for a wide range of weather conditions. In this study, the flow around 23 buildings is simulated. Simulations with different lateral boundary conditions (i.e. symmetric and periodic) are conducted to investigate the limitations that might occur because only a small group of buildings is studied. To fully understand the differences in the local heat island formation mechanisms for the different studied cases, surface temperature, surface heat fluxes, air temperatures, wind speeds and (convective and turbulent) heat fluxes are analysed. Finally, correlations between flow field quantities and the local air temperatures are studied. Based on these correlations an approach is proposed, how the risk of local heat island formation can be estimated based on isothermal CFD simulations.

The structure of the paper is as follows. The generic urban area and the different building height topologies studied in this paper are given in Section 2. In Section 3 the numerical models of BES and

CFD are presented. In Section 4 the simulation results are presented. First the surface temperatures determined and the convective heat fluxes for the different cases are compared. Then air temperatures and total heat fluxes are analysed. Finally, correlations between flow quantities and local heat island intensities are studied and an approach to use isothermal CFD simulations to estimate the local heat island formation risk is proposed. In Section 5 the obtained results are discussed and in Section 6 the conclusions are drawn.

2. Geometries, boundary conditions and computational grids

The study presented in this paper is conducted for a generic urban area consisting of 23 block-type buildings. Six different building height topologies are studied, where the footprints of the buildings and the total volume of the 23 buildings is kept constant while the building heights of the individual buildings are changed (Figure 1). The total building volume is kept constant to assure that for all cases the same building volume is available, meaning also that the average height is kept constant, since the footprint is also kept constant. All building configurations have a plan area density of 0.28 and a frontal area density of 0.34. The individual buildings have a square footprint of 10m x 10 m and a height of 6m – 42m. The buildings are subdivided into different floors, which are 3m high. The building blocks are arranged in a staggered configuration to get complex flow fields, where the building heights can have an important impact on the wind flow patterns. If the buildings would be aligned along the wind direction, the impact of the building geometries on the wind flow would be lower, because a large part of the air would flow through the straight passages between the buildings. The distances between the individual buildings are 30 m in wind direction and 10 m normal to the wind direction. For case A the building heights are decreasing in wind direction. Case B consists of buildings with two different heights. The building heights are varied in both flow directions: along and normal to the wind flow direction. In case C the impact of a high-rise building surrounded by low-rise buildings with uniform building heights on the wind flow structure is studied. Case D is the classical case, where all buildings have the same height. For Case E the building heights are increasing in flow direction and for case F the building heights are first increasing and then decreas-

ing in flow direction.

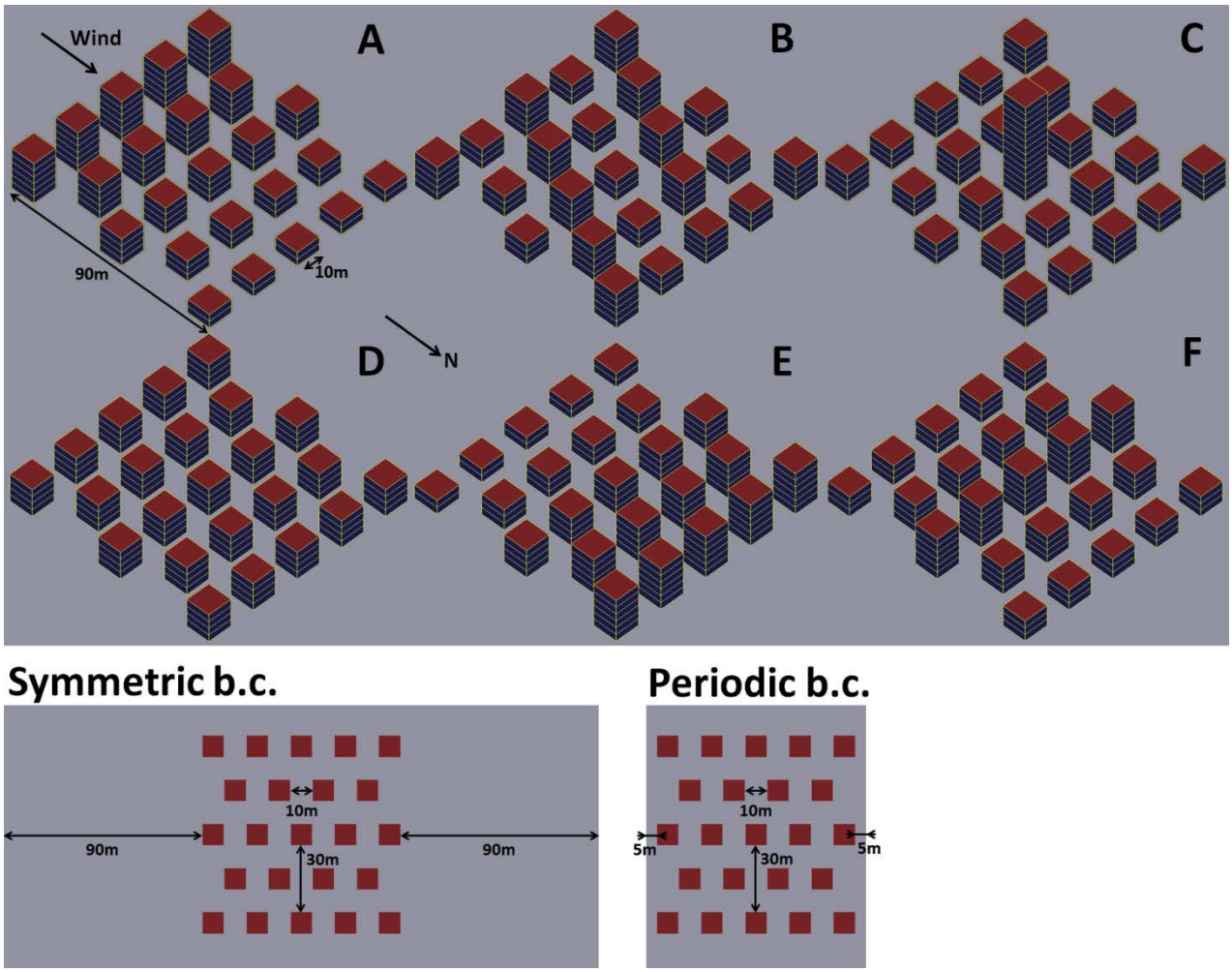

Figure 1: Top: The layout and orientation of the generic urban area under investigation. Cases A-F show the different building height topologies used for the study. Bottom: Footprint of buildings and distances between the buildings and from the buildings to the lateral boundaries of the computational domains used for symmetric and periodic lateral boundary conditions.

All building energy simulations (BES) are conducted for the climate of Zürich (Switzerland). The buildings are modelled as office buildings with corresponding occupancies and internal gains (SIA 2006). Ventilation and infiltration are considered. The glazing (G-value: 0.7, U-value: 1.1 W/m^2K) fraction of the buildings is 50 % and all façades have a solar reflectance of 0.5. The walls have a U-value of 0.18 W/m^2K, the roofs have a U-value of 0.2 W/m^2K and the floors a U-value of 0.25 W/m^2K. External shading devices are used to protect the buildings from solar gains. They close when the solar irradiation on the corresponding façade is > 150 W/m^2 and reopen when it is < 50 W/m^2. Each building consists of one thermal zone. Space heating and space cooling (with no capacity limits) keep the inside air temperature between 20 °C and 26 °C. The building facades are subdivided into smaller parts that are 3 m high (1 floor) and as wide as the buildings. For each of these parts one surface temperature is determined per time step in the BES.

Yearly BES are run with hourly time steps. The CFD simulations are conducted for a selected hour of the year (22nd of July, 3pm, solar zenith angle: 49°, solar azimuth angle: 240°) with a rather high ambient temperature of 28.7 °C, so leading to the condition where heat has to be removed from the urban areas. At the ground and building surfaces, the temperatures as determined by the BES are imposed. This corresponds to a one-way coupling. No two-way coupling is applied, where the surface temperatures would also change dependent on the local wind velocities. A one-way coupling is preferred, while the focus is on a comparison of different cases, when the differences are only due to the differences in the air flow fields and not due to different boundary conditions in the CFD simulations A two-way coupling would lead to more precise predictions of the local surface and air temperatures. However, a lower precision obtained by one-way coupling can be accepted, because the aim of this study is to better understand the local heat island formation mechanisms by increased surface temperatures and not the precise prediction of the local surface and air temperatures in a specific case study. The ground temperature outside the urban areas is set to the ambient air temperature to avoid heating up of the air in the approach flow. The ground surface between the buildings is divided into patches of 10m x 10m. For each of these patches a surface temperature is determined with the BES. For the near-wall modelling, standard wall functions (Launder and Spalding 1974) with no-slip boundary condition were used as a compromise between accuracy and computational cost. The standard wall functions are commonly used for CFD simulations of urban areas, although it is known that the use of wall function can lead to an overestimation of the convective heat flux at the building facades and subsequently to an overestimation of the local air temperatures (Allegrini et al. 2012b). For accurate heat transfer predictions very fine meshes close to surfaces are needed, but with these meshes the surface roughness cannot be accurately modelled, because the cells height has to be much higher than the roughness. Therefore, in this study walls are modelled as smooth walls, what can lead to an underestimation of the connective heat transfer. Since the aim of this parametric study is not an as exact as possible prediction of air temperatures and heat fluxes for a specific case, but the comparison of them for different cases for which the same models with the same limitations are used, the possible over- or underestimation can be accepted.

At the inlet (north of the urban areas) of the computational domain vertical profiles of the mean horizontal wind speed, the turbulent kinetic energy and the turbulence dissipation are imposed for two wind speeds, 1.5 m/s and 5 m/s at 10 m height. The Richardson numbers are 3 and 0.3. For the determination of the Richardson numbers the wind speed at 10 m height and the ambient air temperature are used as reference values. For the surface temperature, the mean surface temperature over all surfaces (see below in Figure 2) is used. Since the surface temperatures for all studied cases are very similar, the mean value of all cases is used here. The air temperature at the inlet is set to the ambient air temperature (28.7 °C). The two wind speeds are chosen to compare a mixed convective with a forced convective condition. The wind direction is for all cases from the North. These profiles represent an atmospheric boundary layer, where the turbulence originates only from friction and shear (Richards and Hoxey 1993):

$$U(y) = \frac{u^*_{ABL}}{k} ln\left(\frac{y+z_0}{z_0}\right) \quad (1)$$

$$k(y) = \frac{{u^*_{ABL}}^2}{\sqrt{C_\mu}} \quad (2)$$

$$\varepsilon(y) = \frac{{u^*_{ABL}}^3}{k(y+z_0)} \quad (3)$$

Here u_{ABL}* is the atmospheric boundary layer friction velocity, y the height above the ground, z_0 the aerodynamic roughness length, k the turbulent kinetic energy, ε the turbulence dissipation rate, U the mean streamwise velocity and C_μ a constant of the turbulence model.

Blocken et al. (2007) showed that the shape of the boundary layer profiles changes in the flow direction when wall functions are used at the ground surfaces. They showed that this change can be limited when the ground surfaces are modelled as rough surfaces. The limitation of this approach is that the roughness height has to be smaller than the distance from the centre point of the wall-adjacent cell to the wall. This requirement conflicts with the fine meshes used in this study. Here the ground surfaces are modelled as smooth walls. Therefore there are small streamwise gradients in the vertical mean wind speed and turbulence profiles. These gradients can however be tolerated, since the study is not on real but generic cases. In this study, the approach flow profiles have to correspond to atmospheric boundary layer profiles, but they do not have to match with a specific measured profile at a certain position.

At the top of the computational domain a symmetry boundary condition is applied. At the outlet an outflow boundary condition is used, which assumes that there are no streamwise gradients at the outlet.

For the main part of this study, symmetric boundary conditions are imposed at the lateral side boundaries. For this case, the computational domain extends 90 m from the building group in lateral directions (see Figure 1). The computational domain extends 90 m upstream and 180 m downstream of the building group. This corresponds to five times the building height of the tallest building upstream and ten times the building height of the tallest building downstream of the urban areas. In vertical direction the domain is six times the building height of the tallest building high. These dimensions are in agreement with best practice guidelines (Franke et al. 2011, Tominaga et al. 2008). For the case C (Figure 1) the dimensions of the computational domain are increased to be in agreement with the best practice guidelines. With this approach of symmetric boundary conditions, we assume that there are no other heated areas in the vicinity of the studied urban area. This might lead to unrealistic results, because in this case cold air can enter the urban areas through the lateral sides and reduce the air temperatures in the studied areas. To study this effect, we run another set of simulations with periodic boundary conditions. For these simulations the computational domain only extends 5 m from the building group in lateral direction (half times the distance between the buildings). With periodic boundary conditions the influence of neighbouring buildings outside the considered domain are modelled. Important is to remark that in this case more space is available between the buildings at the sides than in the middle of the urban areas. For the second and forth row of buildings there is a distance of 15 m between the lateral boundaries and the buildings, while the

distance between the buildings within the urban areas is only 10 m. A consequence is that more cold air can enter the region between the urban areas and the boundaries than between the buildings within the urban areas, what can lead to improved ventilation close to the boundaries (see Figure 1).

Structured grids are built based on a grid sensitivity analysis. The grids are refined towards the walls to resolve the boundary layers. They consist of approximately 8.7 million cells. For the lower wind speed used in this study, the y+ values were < 500; for the higher wind speed, y+ values up to 1500 can be found locally. It was found by conducting simulations with a finer (approximately 15.3 million cells) and a coarser (approximately 4.7 million cells) mesh, that the rather high y+ values did not cause grid dependent results for the wind speeds and temperatures. The grid sensitivity was studied on a horizontal line in the centre between the second and third row of buildings (in wind direction) at a height of 1.75 m above the ground and on a vertical line in the centre of the horizontal line from the ground up to 20 m above the ground. The averaged difference of velocity magnitudes between simulations with the coarse mesh and the mesh used in this study (for case A) was 0.013 m/s on the horizontal line and 0.009 m/s on the vertical line, what are 0.9 % and 0.6 % of the wind speed at 10 m height. For the temperatures the same differences are 0.097 K (6.6 % of the mean local heat island intensity for this case) for the horizontal line and 0.004 K (0.3 % of the mean local heat island intensity for this case) for the vertical line. These differences reduced to 0.006 m/s (0.4 % of the wind speed at 10 m height) and 0.009K (0.6 % of the mean local heat island intensity for this case) for the horizontal line and 0.004 m/s (0.3 % of the wind speed at 10 m height) and 0.003K (0.2 % of the mean local heat island intensity for this case) for the vertical line, when comparing the results between the mesh of this study and the fine mesh. These values are small compared to the differences found between the different cases of this study. The same parameters for the grid generation were used for all configurations and therefore the grid sensitivity analysis gave very similar results for all cases.

All cases of this study are simulated twice: in a first simulation buoyancy is considered and in a second simulation buoyancy is not considered. The impact of buoyancy on the flow fields and air temperatures is studied by comparing the results of the two simulations. We remark that the results from simulations not considering buoyancy do not represent realistic urban flows, but are theoretical results, which are only used to study the impact of buoyancy on urban flows.

3. Numerical solvers

3.1 Radiation and building energy simulation

For the Building Energy Simulation (BES), the program CitySim (Kämpf 2009, Haldi and Robinson 2011 and Robinson 2011) is used. A verification of CitySim was done using the BESTEST (Walter and Kämpf 2015). CitySim is a simulation tool which models the energy fluxes in a city, with a size ranging from a small neighbourhood to an entire city. In CitySim detailed radiation models for solar and longwave radiation are implemented that can account for the radiation exchange between neighbouring buildings, the ground and environment. The Perez All Weather (Perez et al. 1993) and the Simple Radiosity algorithm (Robinson and Stone 2006) are used to compute

hourly irradiations of short and longwave radiation on building surfaces. Multiple iterations for the radiation calculations are performed to achieve consistent results. The heat flow through the walls is determined with a model based on the analogy with an electrical circuit (resistor-capacitor network). The windows are considered as a building surface, but not represented geometrically, therefore no window surface temperature is determined separately and the temperature of the wall is used for the whole façade. For the convective heat transfer coefficients (CHTC) CitySim uses the correlations by McAdams (1954). CitySim uses an hourly timestep, which cannot be changed. With CitySim buildings can be modelled as single- and multi-zone buildings. CitySim also includes HVAC and energy conversion system models (Robinson 2011). CitySim determines the heat balances for all building materials and for the ground. The ground heat balance includes short and longwave radiation and storage of heat as well as heat conduction to the soil. To model the heat storage and heat conduction of the ground, a number of ground layers are defined with the thickness, the heat conductivity and the heat capacity as input parameters.

3.2 CFD

To study the urban microclimate, 3D steady RANS (Reynolds-Averaged Navier-Stokes) CFD simulations are conducted with a realizable k-ε turbulence model with OpenFOAM. For the cases, where buoyancy is considered, the Boussinesq approximation is used. Second-order discretization schemes as well as the SIMPLE algorithm for pressure–velocity coupling are employed. Pressure interpolation is of second order.

4. Results

4.1 Surface temperatures and convective heat fluxes

First results of the BES are presented for the same selected hour of the year as the CFD simulations are conducted. Figure 2 shows the mean surface temperatures averaged over all surfaces within the urban areas for all six studied cases. The temperatures of the building walls, building roofs and the ground are used to determine the mean surface temperatures. The mean surface temperatures are about 17-18°C warmer than the ambient air temperature (used as inlet temperature for the CFD simulations). Due to convective heat exchange between wall and air, these increased surface temperatures lead to increased air temperatures within the urban environment. The mean surface temperatures are similar (45.8 °C -47.0 °C) for all studied building height topologies. The differences are caused by different shadowing effects depending on the geometries of the individual buildings. The differences are rather small, because the distances between the buildings and the footprints of the buildings are kept constant. In addition, the averaged building height is kept constant and therefore decreased shadowing effects of lower buildings are compensated by increased shadowing by higher buildings. Similar results were also found by Allegrini et al. 2017 for realistic building geometries comparing two design options with similar geometries for new buildings in an existing urban neighbourhood. The differences in surface temperatures were found to be larger in winter, when the solar altitude is lower and therefore the shadowing effects are more important (not shown here).

Further, all buildings have the same materials with the same solar properties. The differences might be larger, if different materials would be used for individual buildings. The highest surface temperatures can be found for case E, while the surface temperatures are lowest for case A. For case A the lower buildings receive more shadowing from the higher buildings for most of the day. For case E on the other hand the higher buildings give shadow on the ground outside of the studied urban environment for most of the day.

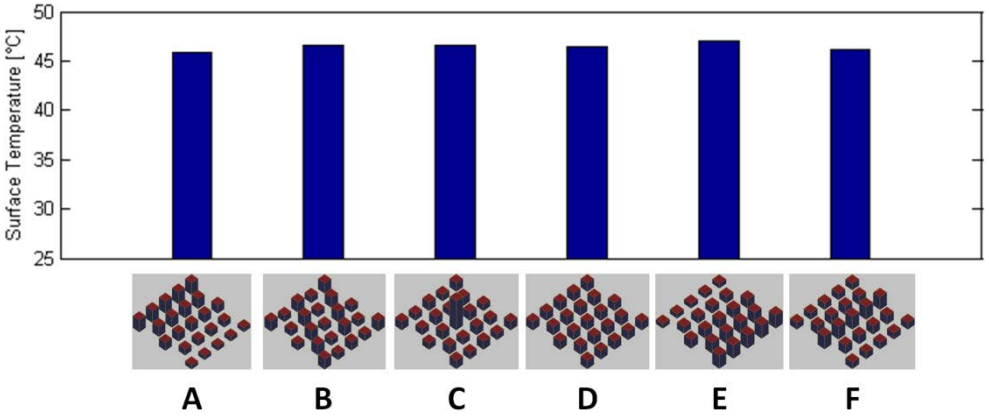

Figure 2: Mean surface temperatures averaged over all surfaces (building and ground surface) within the urban area for the six studied cases.

The surface temperatures from BES are used as boundary conditions in the CFD simulations. The same surface temperatures are used for both approach flow wind speeds and for the simulations considering and not considering buoyancy. In Figure 3 the mean wall heat fluxes per m^2 are given averaged over all surfaces (building walls, building roofs and ground) within the urban areas (determined with CFD). The results are given for the two wind speeds and for simulations with / without buoyancy. The wind speed has the largest impact on the wall heat fluxes. The wall heat fluxes strongly increase as a function of the wind speed. This means that for the higher wind speed cases more heat is transferred from the surfaces to the air in the urban environment. Buoyancy also seems to slightly increase the wall heat fluxes because it increases also the air speeds in urban areas (see later in Figure 6). The impact of buoyancy on the wall heat fluxes is slightly stronger for the low wind speed cases compared to the higher wind speed cases, because for the higher wind speeds the flow is in a more forced convective regime and buoyancy has less influence. The results for the different building height topologies are rather similar. This is due to the fact that the surfaces temperatures (see Figure 2) and wind speeds (see later in Figure 6) are quite similar for the different building height topologies. The differences between the different geometries are slightly higher for higher winds speeds and the cases without buoyancy, because the flow is in a more forced convective regime. For the low wind speed cases, where buoyancy is considered, the differences are very small, because the flow is mainly driven by buoyancy, which has a similar strength for all geometries. For the forced convective cases, higher heat fluxes can be found for building height topologies with tall buildings that face the wind (e.g. cases C, E and F) compared to topologies with lower buildings or buildings that are in the wake of tall buildings (e.g. cases A and D).

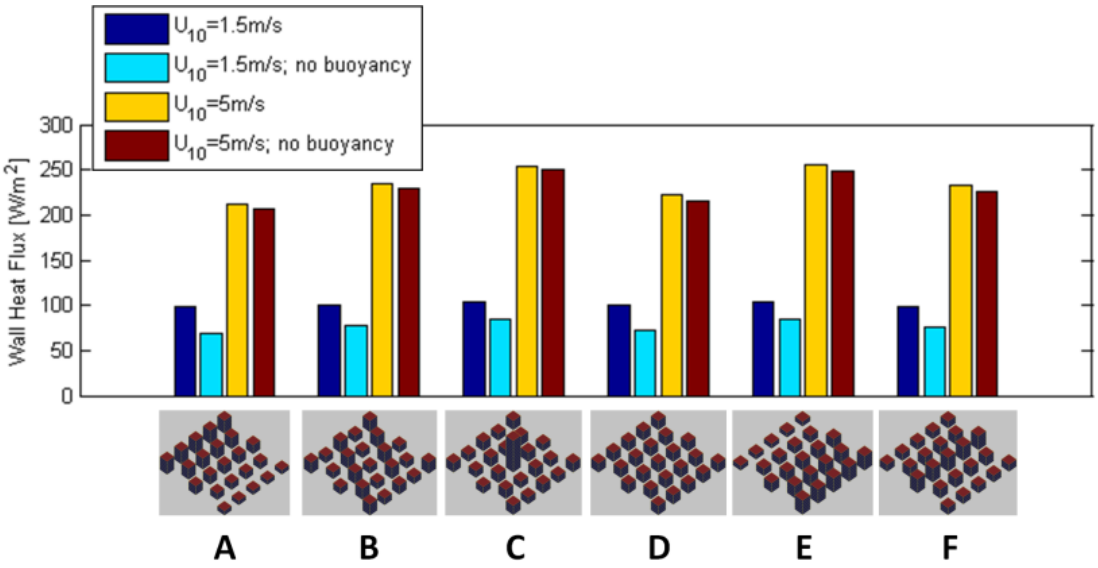

Figure 3: Mean wall heat fluxes averaged over all surfaces (building and ground surfaces) within the urban area for the six studied cases and for the two different wind speeds and simulations considering or not considering buoyancy.

The results of this section show that the amount of heat added from the building surfaces to the air is almost the same for all the different building height topologies, if only the surface temperature boundary conditions are changed for the CFD simulations.

4.2 Air temperatures and flow speeds

In this section mean as well as local air temperatures and mean air flow speeds are analysed. The focus of this section is on the pedestrian thermal comfort. Therefore an air control volume at the pedestrian level, which is 100 m long, 100 m wide and 2 m high, is used for the analysis (Figure 4). The air temperatures at higher levels could also be important for example for building ventilation and space cooling demands of the buildings in the urban environments as air can be taken in from these levels, but these impacts are outside the scope of the paper.

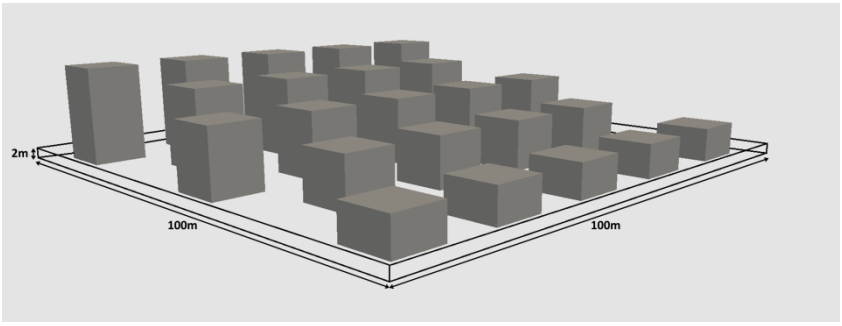

Figure 4: Sketch of the used control volume around one of the building height topologies.

Figure 5 presents mean air temperatures in the control volume defined in Figure 4. The results are given for the two different wind speeds, symmetric (left) and periodic (right) lateral boundary conditions and simulations considering and neglecting buoyancy. The local heat island intensity is defined as the temperature difference between the local air temperature and the ambient air tempera-

ture. Rather strong mean heat island intensities of about 1.5-2.5 °C can be found. Locally the air temperatures are even higher as will be shown later in Figures 8 and 9.

If buoyancy is considered, the heat island intensities are higher for higher wind speeds compared to the lower wind speeds. As discussed in the introduction this effect has already been found by Allegrini et al. (2015a). Higher air temperatures for the higher wind speed case can be due to the lower wind-driven heat removal or due to the higher heat fluxes from the walls to the air. As demonstrated in Figure 3 the heat fluxes from the walls to the air are higher for higher wind speeds, which means they contribute to the higher air temperatures.

If buoyancy is not considered, we observe that the air temperatures are higher for the lower wind speed cases (which is opposite to the case with buoyancy). These higher air temperatures cannot be caused by higher wall heat fluxes, since Figure 3 shows that the wall heat fluxes are lower for the lower wind speed cases. Therefore the reason for the higher air temperatures for the lower wind speed cases for the case without buoyancy has to be the lower wind-driven heat removal.

For the lower wind speed cases the air temperatures are lower if buoyancy is considered compared to the cases without buoyancy. Therefore buoyancy increases the wind-driven heat removal significantly by changing the flow structures. The wall heat fluxes cannot be the reason for the lower air temperatures for the cases with buoyancy, because the wall heat fluxes are higher for these cases.

Based on the observation that the air temperatures are higher for the lower wind speed case without buoyancy, although the surface heat fluxes are lower and based on the observation that buoyancy strongly decreases the air temperatures for the lower wind speed cases, it can be concluded that the air temperatures are lower for the lower wind speed cases due to increased wind-driven heat removal caused by buoyancy (comparing the cases, where buoyancy is considered).

The differences between the results of the symmetric and periodic boundary conditions are rather small. For the higher wind speed cases the air temperatures are very similar. For the lower wind speed cases the air temperatures for the periodic boundary conditions are a bit higher. Due to buoyancy, more cold air will be entering from the lateral sides of the building array (which do not coincide with the lateral boundaries of the computational domain, but have a 5 m distance from them) into the urban environments of the lower wind speed cases compared to the higher wind speed cases. For the simulations with periodic boundary conditions there is less cold air available to enter from the lateral sides. This impact is not as large as it might be expected since there is still cold air entering at the roof level for the lower wind speed cases with periodic boundary conditions. This conclusion might change, if additional buildings are added to model an infinite wide array of staggered buildings. In that case, there are no zones, where cold air can so easily enter between the buildings.

Comparing results for the different building height topologies, it can be seen that the air temperatures are lower for cases, where taller buildings (cases C and F) can deflect the colder air from above the urban environment to the pedestrian level, but these differences are rather small. The

lowest air temperatures can be found for case C with a high-rise building. For cases A and D the temperatures are highest. For case A the tallest buildings are at the upstream part of the urban area deflecting the cold air upwards. For case C all the buildings have the same height and therefore the mixing of the air at the roof level and the cold air entering the pedestrian level is reduced.

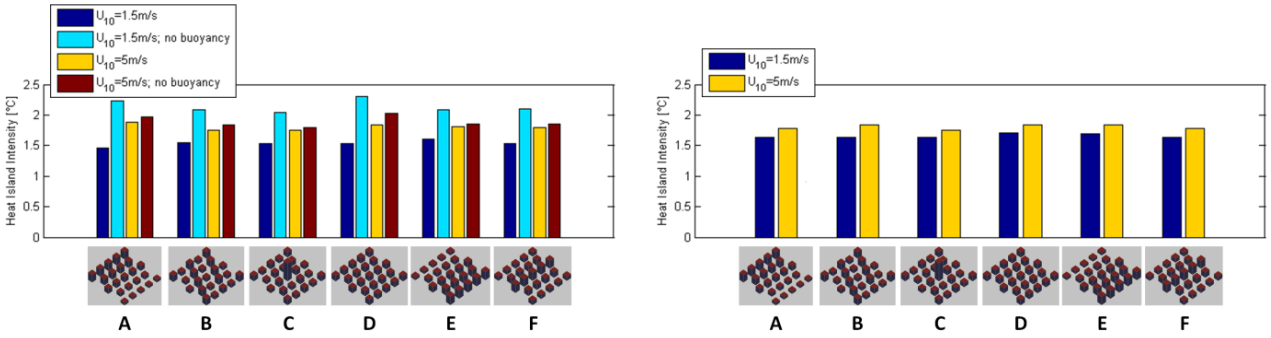

Figure 5: Mean heat island intensity in the control volume for the six studied cases. The heat island intensity is defined as the temperature difference between the local air temperature and the ambient air temperature. Results are given for the two different wind speeds, symmetric (left) and periodic (right) boundary conditions and simulations considering or not considering buoyancy.

Besides the air temperature also the air speed has a strong impact on the thermal comfort of pedestrians in an urban environment. Figure 6 shows the mean air speeds inside the control volume defined in Figure 4. The results are given for the same cases as for the mean air temperatures in Figure 5. The air speeds are higher for higher approach flow wind speeds. Buoyancy also increases the air speeds in the urban areas. The air speeds are higher for the periodic cases, because air is forced to flow in between the buildings, since air cannot flow around as in the symmetric case. Comparing the results between the urban areas with different building height topologies, it can be seen that for the cases with high average air temperatures, the average air speeds are low and vice versa (Figure 7). For higher air speeds the air temperatures are lower, because more heat can be removed by convection.

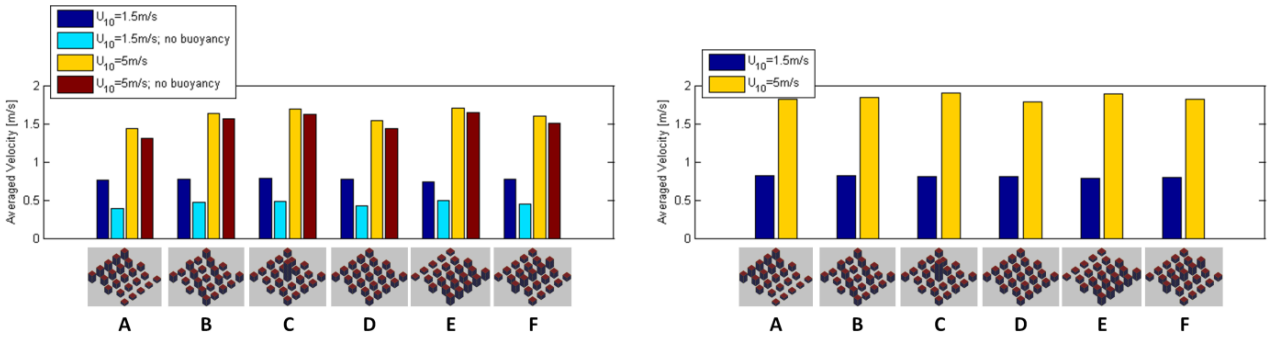

Figure 6: Mean flow speeds in the control volume for the six studied cases. Results are given for the two different wind speeds, symmetric (left) and periodic (right) boundary conditions and simulations considering or not considering buoyancy.

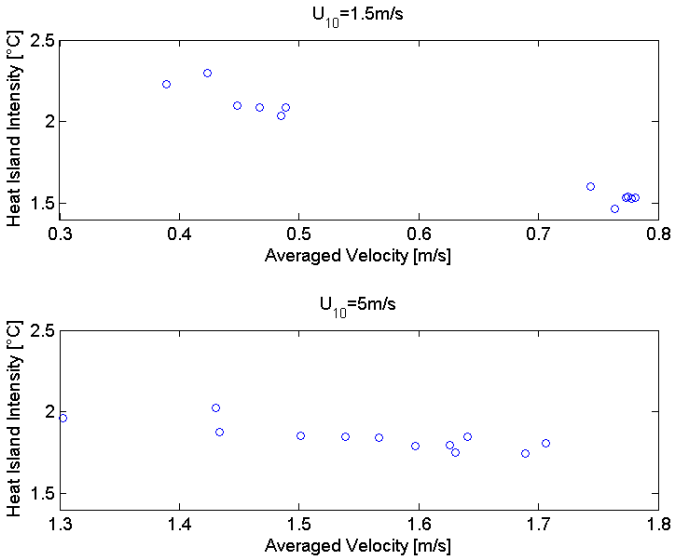

Figure 7: Mean heat island intensity in the control volume for the six studied cases as a function of the mean flow speeds in the same control volume for the same cases considering and not considering buoyancy (using symmetric boundary conditions).

The analysis of the mean surface temperatures, wall heat fluxes, air temperatures and wind speeds leads to the conclusion that the lower temperatures for mixed convective conditions are mainly caused by the increased heat removal due to buoyancy.

Air temperatures in urban areas can strongly vary from place to place, referred to as local heat islands. For the pedestrian comfort local values are more important than average values. Therefore besides the average air temperatures also local air temperatures are studied in this section. Figure 8 shows false-colour plots of the local heat island intensities, defined as the temperature difference between the local air temperature and the ambient air temperature for two wind speeds at a height of 1.75 m. For all cases strong local heat islands of more than 3°C can be found. The locations of the local heat island strongly depend on the building height topology. For case A there are large wake regions downstream of the tall buildings. The warmer air gets trapped in these wake regions, what leads to increased air temperatures in the downstream parts of the urban area. In case B, the buildings with two different heights, where slightly taller buildings are spread over the whole urban area. Compared to case A the areas of the local heat islands are smaller. In case B, more cold air enters the urban area through the rooftop layer, what leads to regions with colder air further downstream of the urban area. A clear effect of the high-rise building can be found in the centre of the urban area of case C. The temperatures around the high-rise building are significantly lower compared to the temperatures around the neighbouring buildings. The high-rise building deflects air at lower temperature from above the roof level of the low-rise buildings into the urban environment. Therefore high-rise buildings lead to a local decrease in air temperatures in urban areas, but at the same time the local flow speeds increase (not shown here). Case E has the same building geometries as case A, but the wind direction is different. As case A also case E shows large local heat islands with high intensities. For case E more air is deflected into the urban area compared to case A, but the down-

wards motion of the air does not allow the removal of warmer air through the top. For case F lower air temperatures can be found in the regions, where the building heights are increasing and higher air temperatures can be found, where the building heights are decreasing.

For the lower wind speed cases the differences between the different building height topologies is smaller. For low wind speeds the air heats up close to the buildings and due to buoyancy it is transported upwards resulting in the removal of warm air (see also Figure 10). The local heat islands are mostly elongated areas in flow direction between the individual buildings.

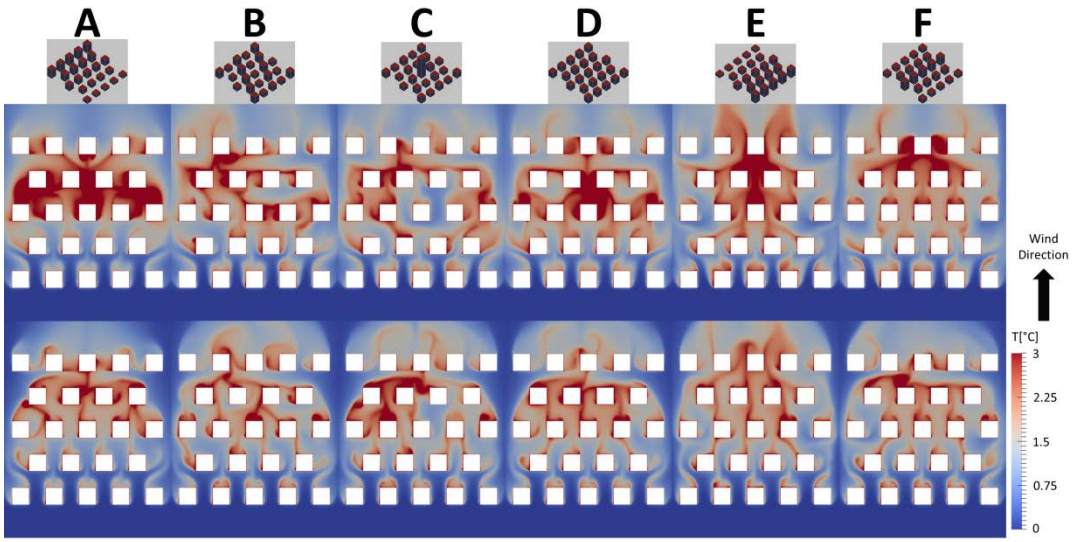

Figure 8: False-colour plots of the local heat island intensities, defined as the temperature difference between the local air temperature and the ambient air temperature at 1.75m height for different wind speeds (top: U_{10} = 5 m/s; and bottom U_{10} = 1.5 m/s) and building height topologies. Results are given for symmetric boundary conditions. Buoyancy is considered.

In Figure 9 the same results are presented for periodic lateral boundary conditions, where the results in Figure 8 are for symmetric lateral boundary conditions. For the periodic boundary conditions the air temperatures at the lateral sides of the urban areas are higher, because there is less cold air available to enter the urban areas through the sides. In general the locations of the local heat islands are similar for the symmetric and periodic boundary conditions. Small differences can be found due to differences in the flow fields. Differences can mainly be seen for cases, where the flow is not that strongly influenced by strong changes in buildings heights within the urban area (e.g cases B and D). Based on the results of this study it can be concluded that the lateral neighbourhood does not have a strong impact on the local temperatures in the urban area. This might be different when the lateral boundaries are defined in a different way or when the air temperatures in lateral directions are strongly changing (i.e. much higher temperatures in lateral neighbourhoods).

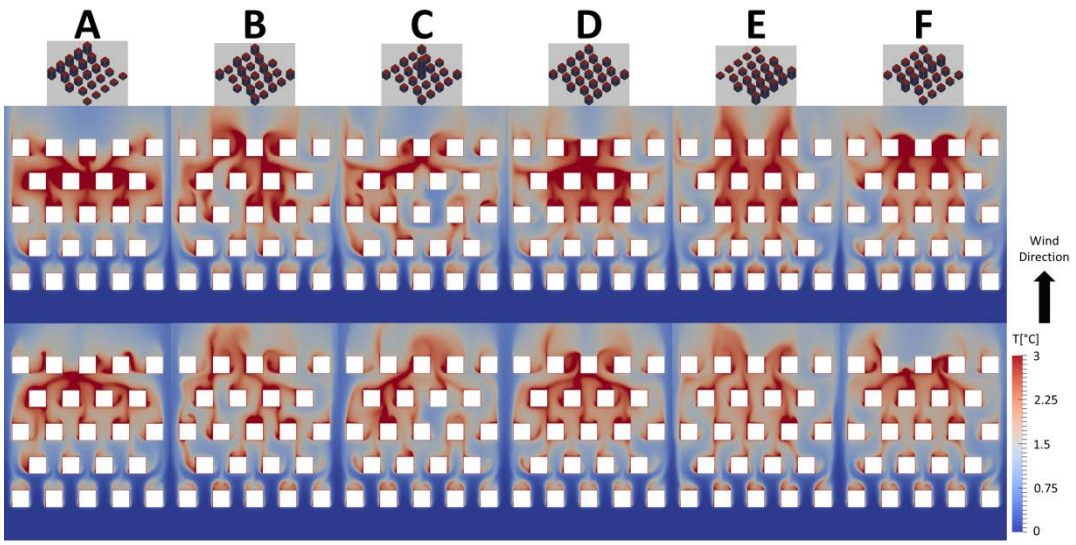

Figure 9: False-colour plots of the local heat island intensities, defined as the temperature difference between the local air temperature and the ambient air temperature at 1.75m height for different wind speeds (top: U_{10} = 5 m/s; and bottom U_{10} = 1.5 m/s) and building height topologies. Results are given for periodic boundary conditions. Buoyancy is considered.

Building height topology is found not to have a strong impact on the mean air temperatures for cases with the studied building footprints and packing density, but it influences the locations and dimensions of local heat islands. Additional analysis showed that also the minimum and maximum temperatures are very similar for the different cases (not shown here). Further, also the total areas, where the temperature is above a certain value, are similar (also not shown here). Finally, it was shown in this section that adequate conclusions for the urban microclimate can be drawn from simulations with a small group of buildings as long as all important flow features (e.g. largest eddies) can be resolved, because there is no strong impact of buildings at the lateral sides on the mean as well as local air temperatures.

4.3 Vertical air and heat exchange

To improve the microclimate in urban areas, it has to be understood how (local or urban) heat islands form, and how this formation can be mitigated. The flow structures have to be studied in detail, because wind can transport as well cold as warm air and can therefore have a cooling or a heating potential. Further, it should be noted that heat is not only transported by convection, but also by turbulence. Therefore convective and turbulent heat fluxes have to be studied in more detail to understand how heat is removed from urban areas. Allegrini et al. (2015b) analysed the convective and turbulent heat fluxes through boundaries of a control volume around small groups of buildings. Here the same definitions for the heat fluxes through a plane are used as in Allegrini et al. (2015b). The turbulent heat fluxes (here including the heat conduction) and the convective heat fluxes are determined as follows:

$$Q_{conv} = \int u(T - T_\infty) c_p \rho \, dA \tag{4}$$

529 $$Q_{turb} = \int \alpha_{eff} \frac{\Delta T}{\Delta n} c_p \rho \, dA \quad (5)$$

530 Here Q_{conv} is the convective heat flux, u the velocity normal to the plane, T the temperature, T_∞ a
531 reference temperature (here mean temperature in the control volume defined in Figure 4 or later in
532 Figure 14), c_p the heat capacity, ρ the density, α_{eff} the effective thermal diffusivity consisting of the
533 thermal diffusivity and the turbulent thermal diffusivity and n the direction normal to the plane.

534 In Allegrini et al. (2015b) heat fluxes were only studied at the boundaries of the urban areas. In this
535 study we analyse also the local heat fluxes. For the determination of the convective heat fluxes, the
536 average temperature in the large control volume defined in Figure 4 is taken as reference tempera-
537 ture. Therefore the results show how much heat is added or removed from the control volume. Lo-
538 cally it can still have another effect, because the temperature might locally be much higher or lower
539 than the average temperature inside the control volume. A cooling effect by convection can have
540 two causes: either cold air is transported through a plane into the control volume, or warm air is
541 transported though a plane out of the control volume to the surrounding environment. On the con-
542 trary, warm air that enters the control volume or cold that leaves the control volume can have a
543 heating effect.

544 Before studying the heat fluxes, first velocities normal to the top plane of control volume are pre-
545 sented to later compare the air flow directions with the heat fluxes and study which type of cooling
546 or heating effects are present. In Figure 10, the vertical velocity components are given for the dif-
547 ferent studied cases at a height of 2 m, where positive values indicate flows upwards and negative
548 values flows into the control volume. Very complex flow structures can be found for all studied
549 cases. For all cases there are rather strong upwards motions upstream and between the buildings of
550 the first row of buildings, because a large part of the air is flowing over the urban areas instead of
551 through the urban areas. At the windward wall of the first row of buildings, there are downwards
552 motions. These motions are stronger when taller buildings are present. Stronger downwards mo-
553 tions can be found for buildings, which are not or just partly in a wake of upstream buildings.
554 Strong downwards motions can for example be found at the high-rise building of case C or for
555 buildings at the lateral boundaries of the urban areas (e.g. for case E or F). Comparing Figure 9 and
556 10 it can be seen that high downwards motions mostly coincide with regions with lower air temper-
557 atures. Upwards motions can mainly be found in the wake of buildings or between two rows of
558 buildings. After the first row of buildings the upwards air motions often coincide with increased air
559 temperatures. Differences between the lower and higher wind speed cases can be found. For the low
560 wind speed cases the influence of tall buildings is less pronounced and more upwards motions ap-
561 pear caused by buoyancy. Also the upwards motions are relatively stronger in comparison with the
562 downstream motions for the low wind speed cases.

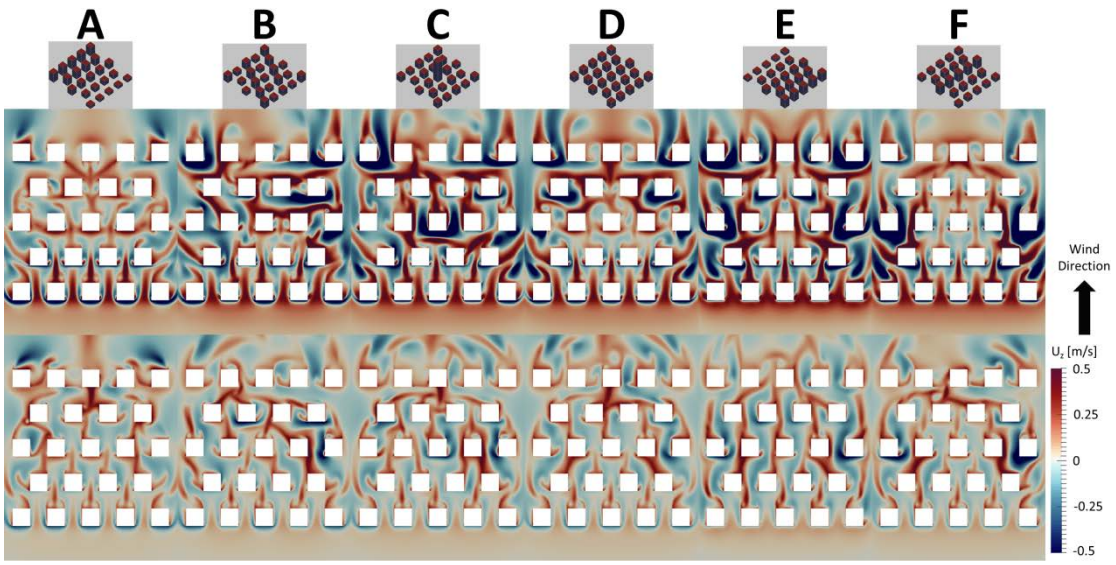

Figure 10: False-colour plots of the vertical velocity component at 2 m height for different wind speeds (top: U_{10} = 5 m/s; and bottom U_{10} = 1.5 m/s) and building height topologies. Results are given for symmetric boundary conditions. Buoyancy is considered.

In Figure 11 the convective heat fluxes at the horizontal top plane of the control volume are given. Positive values indicate a cooling effect (blue colour), while negative values a heating (red colour). The mean air temperature inside the control volume is used as reference temperature for Equation 4. For all cases there is a heating effect at the first row of buildings. This heating effect is due to cold air that moves upwards (compare with Figure 10). This cold air is then not available anymore to cool the urban area and therefore leads to a relative heating effect. Further downstream the heating and cooling effects are very locally distributed. As discussed above, upwards air motions can also lead to a cooling effect. This can for example be seen in the red box in Figure 11 for case F. Here strong cooling effects can be found (blue colours in red box). Figure 10 shows that in these locations there are upwards air motions. Therefore warm air is leaving the control volume through the top plane. Around the high-rise building in case C, a cooling effect due to cold air entering the control volume through the top plane can be found (black box in Figure 11). Similar effects can be seen at other locations, where there are strong downwards air motions. In a few regions there are also heating effects due to warm air moving downwards (orange box in Figure 11).

For the lower wind speed cases the convective fluxes are lower. The cooling effects are mainly due to warm air moving upwards and less due to cold air moving downwards. Comparing Figures 9-11 it can be seen that the areas with positive convective heat fluxes mostly coincide with the areas, where warm air is moving upwards. Therefore, there is a strong impact of buoyancy on the heat removal. The impact of high-rise buildings on the heat removal is rather limited for the lower wind speed cases. For example only a weak cooling effect can be seen close to the high-rise building of case C.

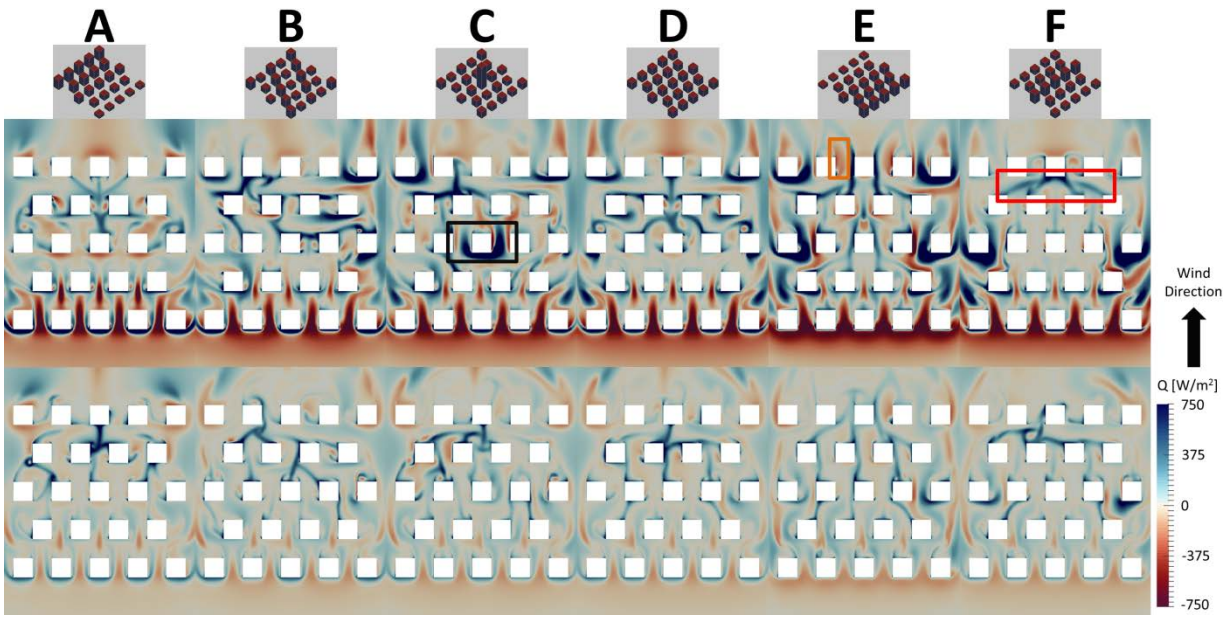

Figure 11: False-colour plots of the vertical convective heat flux component at 2 m height for different wind speeds (top: U_{10} = 5 m/s; and bottom U_{10} = 1.5 m/s) and building height topologies. Results are given for symmetric boundary conditions. Buoyancy is considered.

Figure 12 shows the turbulent heat fluxes at the horizontal top plane of the control volume. Negative values indicate a cooling effect (blue colour), while positive values a heating (red colour). The turbulent heat fluxes are weaker compared to the convective heat fluxes. This corresponds to the findings of Allegrini et al. (2015b), who found that the turbulent heat fluxes are mainly important in shear layer regions. The turbulent heat fluxes have mostly a cooling effect, because the gradient in air temperatures is mostly negative in vertical direction (increasing air temperature towards the ground). Only at very few locations the air temperature gradient is positive (decreasing towards the ground) resulting in a heating effect due to turbulence. As the convective heat fluxes, also the turbulent heat fluxes are larger for the higher wind speed cases.

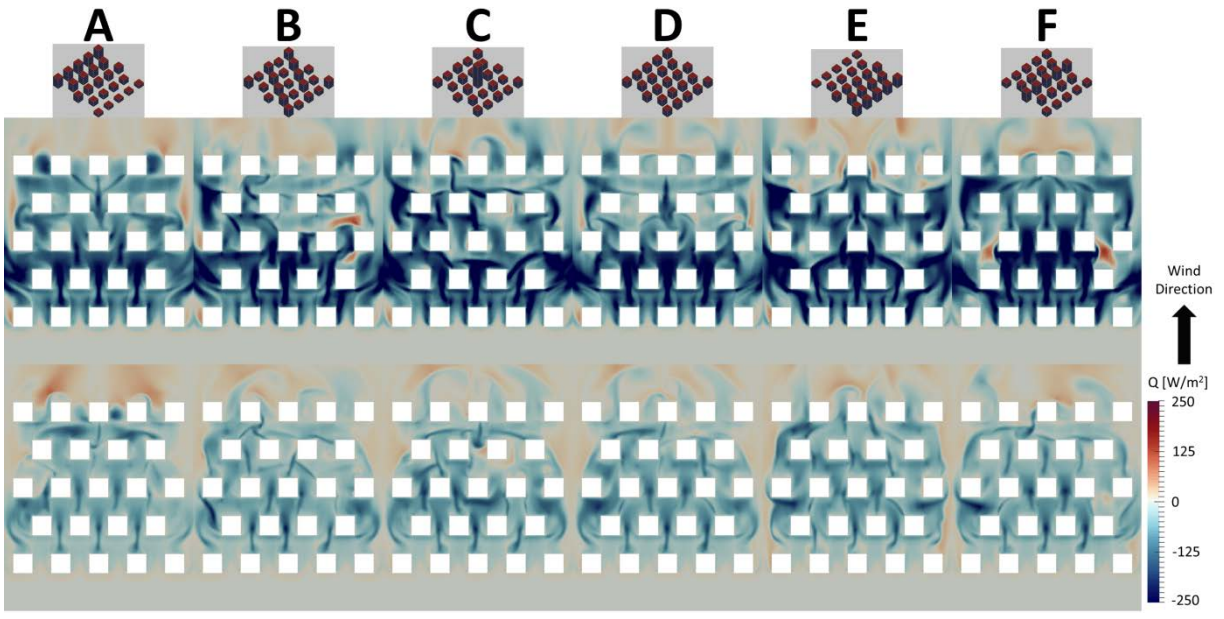

Figure 12: False-colour plots of the vertical turbulent heat flux component at 2 m height for different wind speeds (top: U_{10} = 5 m/s; and bottom U_{10} = 1.5 m/s) and building height topologies. Results are given for symmetric boundary conditions. Buoyancy is considered.

The results in this section show the complexity of how heat is transported in urban areas. This illustrates the difficulty to understand or predict the formation of local heat islands without having detailed flow field information from for example CFD simulations.

4.4 Impact of buoyancy on the flow fields

As discussed above buoyancy has a strong impact on the heat removal potential for the low wind speed cases. Buoyancy increases the convective heat removal through the top plane of the urban areas, due to the vertical motions induced by buoyancy. As an example, we present in Figure 13 the vertical velocity components on a vertical plane for case C for different wind speeds. The flow patterns for low and high wind speed cases are very different with or without buoyancy. For the lower wind speed case, smaller flow structures can be found. These small convective cells, which are caused by buoyancy, increase the mixing with the flow above the buildings and therefore increase the heat removal potential. If buoyancy is not considered, the flow structures are similar as for the high speed case due to Reynolds number independency. If buoyancy is considered, the up- and downwards motions have similar strength for both wind speeds. Without buoyancy the up and downwards motions are both significantly lower. Therefore, buoyancy increases the heat removal for low wind speeds cases. This has a positive effect on the local microclimate.

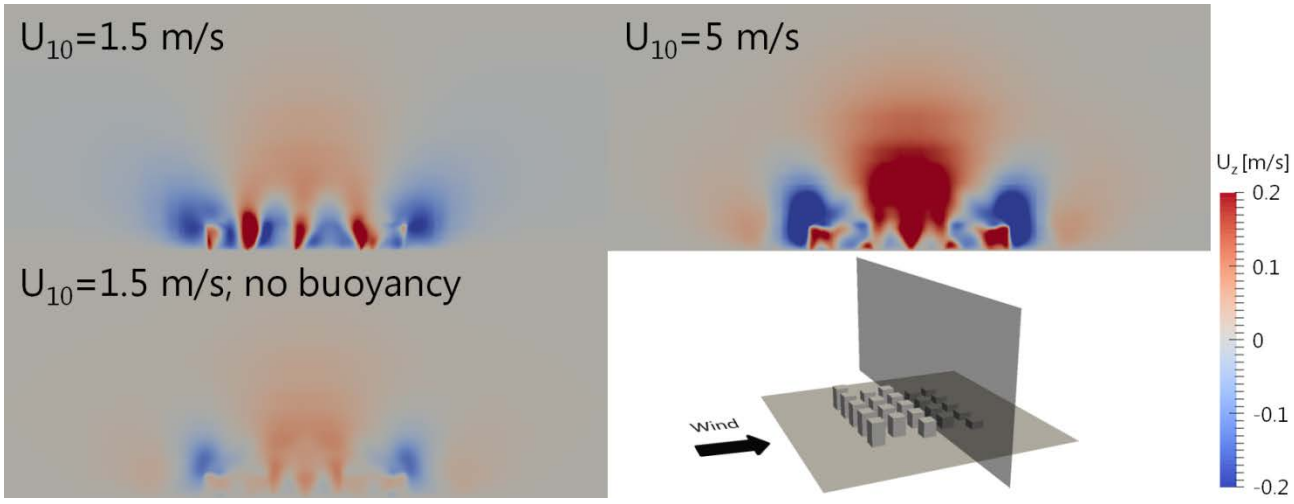

Figure 13: False-colour plots of the vertical velocity component in the centre between the 3rd and 4th row of buildings for case A. Results are given for two wind speeds considering buoyancy and for the lower wind speed also without buoyancy.

4.5 Prediction of local heat island formation risk based on correlations

In the sections above the formation of local heat islands was discussed. With the detailed information of CFD simulations, the reason for particular locations of local heat islands can be studied and explained in detail by analysing the turbulent and convective heat fluxes. In a next step, it

would be advantageous to have an easy approach to predict regions, where the probability of local heat island formation is high without having to run coupled BES-CFD simulations. Coupled BES-CFD simulations are time consuming to setup and run and a large number of input parameters are needed. Especially detailed material properties of the buildings and pavements are not known in early design stages of new buildings or urban neighbourhoods. Nevertheless, this is the stage where urban microclimate studies should be carried out to still be able to implement local heat island mitigation measures. The choice of materials with certain properties might also be part of the local heat island mitigation measures. Therefore, it would be advantageous to be able to find critical regions, where the risk of local heat island formation is high based on less time consuming isothermal CFD simulations. Therefore, in this section we look for correlations between the risk of local heat island formation and flow quantities that can be extracted from isothermal CFD simulations (RANS). Equations 4 and 5 describe the mechanism for the removal of sensible heat from a control volume (e.g. region in an urban area). Sensible heat can be removed efficiently by convection, if the wind speeds normal to the boundaries of the considered volume are high (Equation 4). In that case only small temperature differences are needed between the control volume and the neighbouring environments to already remove a large amount of sensible heat from the control volume. Sensible heat can also be removed with turbulent thermal diffusion, when the effective thermal diffusivity is high (Equation 5). When the velocities normal to the boundaries are low and the turbulent thermal diffusion is also low, the air temperature in the control volume increases, as well as the temperature gradients between the control volume and the surrounding environment resulting in a higher potential to remove sensible heat from the control volume by convection (Equation 4) and turbulent thermal diffusion (Equation 5). Therefore one can reason that the local heat island intensity has to be a function of the heat gains to the control volume (by convection, thermal diffusion, wall heat transfer etc.), but also depends on the air velocities normal to the boundaries of the control volume and the effective thermal diffusivity at the boundaries of the control volume. The heat gains to the control volume can be influenced in the early design stage for example with the material choice of buildings and pavements. Using for example highly reflective paints can reduce the sensible heat gains due to absorption of solar radiation. The air velocities can be determined with isothermal CFD simulations (for forced convective flows, no buoyancy). The effective thermal diffusivity is the sum of the laminar and turbulent thermal diffusivities. In urban flows the laminar thermal diffusivity is negligible compared to the turbulent thermal diffusivity. The turbulent thermal diffusivity can be determined using the turbulent Prandtl number (Pr_t) and the momentum eddy diffusivity or turbulent eddy viscosity (ν_t):

$$\alpha_t = \frac{\boldsymbol{\nu}_t}{Pr_t} \tag{6}$$

The momentum eddy diffusivity is modelled in RANS simulations, if a k-ε turbulence model is used or can be determined using the Boussinesq eddy viscosity assumption for other turbulence models. Based on the above reasoning, we may assume that there should exist a correlation between the local heat island intensity normalized by the sensible heat gains of the control volume and the

volume flow rates from the control volume to the environment (integral of the velocities normal to the boundaries over the boundaries of the control volume) and the turbulent diffusivity integrated over the boundaries of the control volume. The normalized local heat island intensity can be understood as a measure for the risk of local heat island formation. For high normalized heat island intensities the air temperatures in the control volume will increase already with low sensible heat gains. If the normalized heat island intensity is low, there is a low risk for local heat island formation, because high sensible heat gains are needed to significantly increase the local air temperatures. To confirm the existence of the proposed correlations, we analyse the heat island formation risk in eight small (10 m x 10 m x 2 m) control volumes around a building block (Figure 14).

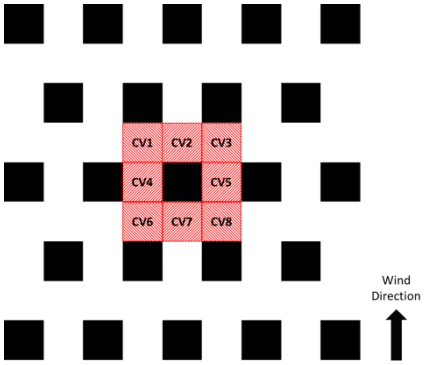

Figure 14: Sketch of the 8 small control volumes (CV1-CV8) used in this section.

In Figure 15 we give the correlation between the local heat island intensity normalized by the sensible heat gains inside the control volume and the volume flow rates at the boundaries and the integrated turbulent thermal diffusivity. The sensible heat gains are the sum of the convective heat fluxes, the turbulent heat fluxes from the environment to the control volume and the heat fluxes from the walls to the control volume. Each circle in Figure 15 presents the results for one control volume (CV1-CV8) and one wind speed case. Results are included for the two wind speeds (1.5 m/s and 5 m/s) considering buoyancy and for the case with the lower wind speed (1.5 m/s) neglecting buoyancy and all building height topologies. The results of the higher wind speed neglecting buoyancy are not presented, because they are very close to the results, where buoyancy is considered. Clear correlations between both flow quantities and the normalized local heat island intensities can be found showing a power law relationship (linear in log-log plot). This is remarkable result, because we notice that the results in Figure 15 represent a very wide range of flow structures and air temperatures. Based on the observed correlation, it can be concluded that when the flow structures and the location of the heat sources are known, it is possible to qualitatively predict the locations of local heat islands. We remark that logarithmic scales are used in Figure 15 (a and b) and therefore for low values of the volume flow rates and turbulent thermal diffusivities small changes of these parameters lead to large changes in the normalized local heat island intensities.

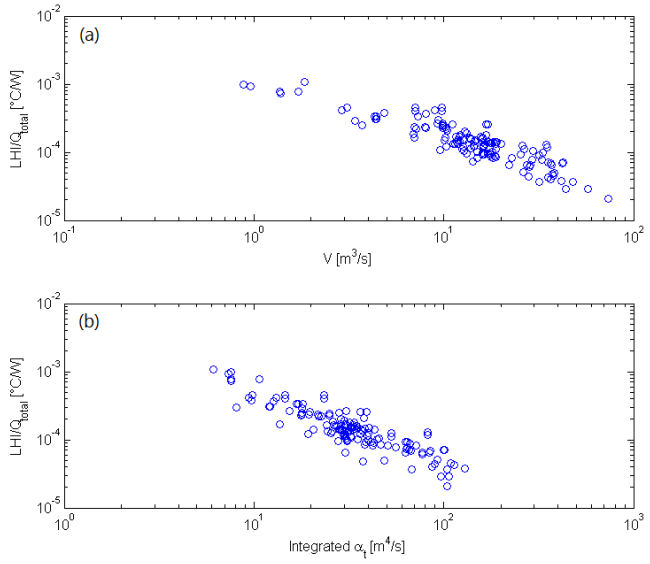

Figure 15: Local heat island (LHI) intensity normalized by the sensible heat gains in the control volume as a function of the volume flow rates at the boundaries (a) and the integrated turbulent thermal diffusivity (b).

In Figure 16 results of the different quantities for the 8 control volumes are presented for case E (uniform building heights). Let's discuss the results for CV7 in more detail. For all three cases (two wind speeds and lower wind speed without buoyancy) the values of the volume flow rates and integrated turbulent thermal diffusivities are high. Since there is a correlation between these two values and the normalized local heat island intensity, also the normalized local heat island intensities are low. This means that there is a low risk for local heat island intensity formation. Even with high sensible heat gains the temperatures will not increase strongly. Finally it can be seen that also the local heat island intensities are low in CV7. For the lower wind speeds cases, the values of the volume flow rates and integrated turbulent thermal diffusivities are much lower without buoyancy compared to the case with buoyancy. This leads to the higher risk for local heat island formation and in the studied cases to the higher local heat island intensities. When buoyancy is considered the risk for local heat island formation is similar for the two studied wind speeds. The local heat island intensities are higher for the higher wind speed case, because the sensible heat gains are higher due to the higher wall heat fluxes (see Figure 3).

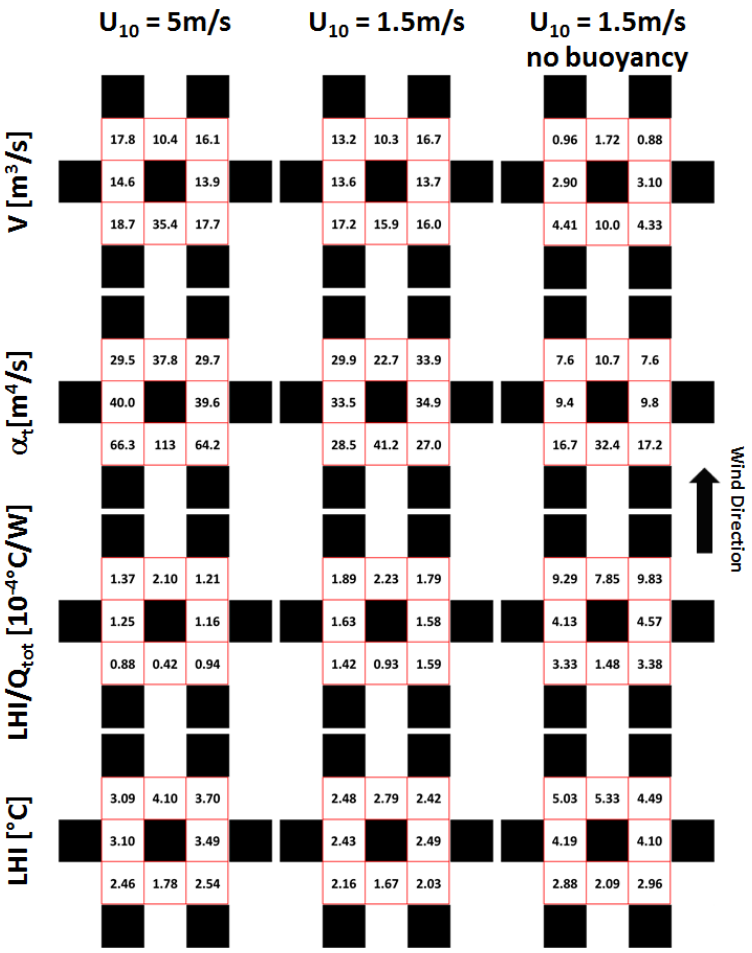

Figure 16: Volume flow rates, integrated turbulent thermal diffusivities, normalized local heat island intensities and local heat island intensities for the different control volumes. Results are included for the two wind speeds (1.5 m/s and 5 m/s) considering buoyancy and for the case with the lower wind speed (1.5 m/s) neglecting buoyancy. The results are only given for the case with uniform building heights (D).

The results presented in Figures 15 and 16 confirm that the risk of local heat island formation can be estimated based on the volume flow rates and the turbulent thermal diffusivity, which can be extracted from isothermal CFD simulations. Based on these new insights on the physics of local heat island formation, we propose the following new approach to find in an efficient way local heat island mitigation measures:

1. Run isothermal CFD simulations
2. Divide the urban area into small control volumes
3. Determine the volume flow rates and turbulent thermal diffusivities at the boundaries
4. Find control volumes with low values for the volume flow rates and thermal diffusivities. These are the regions with high local heat island formation risk due to the high normalized local heat island intensities.

5. To mitigate the local heat island formation in the early design phase, adjust the building geometries to increase the volume flow rates and turbulent thermal diffusivities and lower the normalized local heat island intensities
6. Rerun isothermal CFD simulations with improved geometries
7. Minimize the sensible heat gains in control volumes with high local heat island intensities (e.g. use materials with albedo, reduce traffic, reduce exhaust of warm gases from industry or air conditioning systems) or create sensible heat sinks (e.g. vegetation). Note that if the risk of local heat island formation is minimized for all control volumes, the sensible heat gains from convection and turbulent thermal diffusion are automatically minimized.
8. Propose local heat island mitigation measures to urban planners or architects

5. Discussion

In this paper the impacts of different building height topologies and buoyancy on the local microclimate in urban areas were studied with coupled BES-CFD simulations. The study shows interesting new results on the formation of local heat islands, but to draw more general conclusions a larger number of simulations is still needed. A number of simplifications were made in this study. Only one wind direction was considered. Possible impacts of traffic and vegetation on the microclimate were neglected. The neighbourhood of the studied urban areas was modelled in a very simplified way. In reality there can be complex interactions with the surrounding of the studied urban environment. These complex interactions should be considered. Especially the larger scale urban heat island effect should be taken into account. Further only staggered arrays of block type buildings were modelled here. Also more complex building geometries should be studied. These building geometries could also include building details as for example balconies.

This study was conducted for just one climate (Zürich, Switzerland). It is assumed that the conclusions are also valid for other climates, because the physics of the heat exchange mechanisms remain the same.

The understanding of the heat exchange mechanisms in urban areas could be improved by running time resolved large eddy simulations (LES). In this study, no LES are conducted due to its high computational costs. For this study especially fine meshes would be needed close to the building and street surfaces and in shear layer regions to accurately predict the heat fluxes.

A two-way coupling, where the convective heat transfer coefficients as determined from CFD are used in BES, could improve the predicted building surface temperatures.

Finally an approach is proposed to predict the risk of local heat island formation based on isothermal CFD simulations. This approach can only be used for forced convective flows. For the cases presented in this study, the local heat island intensities are higher for the forced convective cases and therefore the local heat island formation risk could be estimated using isothermal CFD simulations.

6. Conclusion

The local microclimates for six different urban topologies were studied using steady CFD (computational fluid dynamics) and building energy simulations (BES). The urban areas consisted of 23 buildings and the same building footprints, building locations and total building volumes were used for all six urban topologies. Only the building heights were varied for the different topologies. We found that the mean surface temperatures are similar for the different topologies. The air temperatures inside the urban areas are strongly dependent on the approach flow wind speeds. Buoyancy has a strong impact on the local air temperatures. For low wind speeds, results of simulations, where buoyancy is not considered, show strongly increased temperatures compared to the simulations considering buoyancy. If buoyancy is considered (or neglected) and the same approach flow wind speeds are used for all cases, the mean air temperatures are similar for different building height topologies, but strong differences in the local air temperatures can be found.

The mean microclimate in the urban area is found not to change a lot for different building height topologies when the total volume of the buildings, the footprints and the distances between the buildings are kept constant. However, the local microclimate can vary a lot dependent on the urban topology. For example high-rise buildings can deflect cold air from higher levels down to the pedestrian level leading to a local cooling effect. For higher wind speeds the building geometries are more important than for low wind speeds. For low wind speeds the flow is mainly driven by buoyancy, which introduces a heat removal, because it increases the ventilation of the urban areas and can therefore lower the average and local air temperatures. With buoyancy small convective cells increase the mixing with the flow above and can bring cold air into the urban areas. Due to buoyancy not only more heat can be removed, what leads to lower air temperatures, but also the local air speeds are increased leading to a better thermal comfort for pedestrians.

The analysing the convective and turbulent heat fluxes gives insights in the physics of local heat island formation. Convective as well as turbulent heat fluxes can contribute to cooling or heating of urban environments depending on the temperature distribution. For example, cold air removed from an urban environment as well as warm air added to an urban environment due to turbulence or convection can have a heating effect. Therefore, convective and turbulent heat fluxes have to be studied carefully together with the flow fields and temperature fields to be able to understand the formation of local heat islands.

Finally, an approach is proposed based on which the risk of local heat island formation can be estimated based on isothermal CFD simulations. A correlation was found showing that the normalised (by the sensible heat gains) increase in local air temperature is linked to the air volume flow rates (convective exchange) and local thermal diffusivity (turbulent exchange). This means that with higher air volume rates and higher thermal diffusivities more heat can be removed from the urban environment leading to lower risks of local heat island formation. Therefore, for a given heat gain of a urban control volume, the local heat island formation risk of an urban environment can be estimated directly from the flow field, when the velocities and momentum eddy diffusivity are known

(using the turbulent Prandtl number). Building geometries can based on this information improved to reduce the local heat island formation risk or measures to minimize the sensible heat gains have to be applied in regions, where the risk cannot be reduced.

Acknowledgments

Funding by CCEM (Urban Multi-scale Energy Modelling project and Synergistic Energy and Comfort through Urban Resource Effectiveness project) is gratefully acknowledged.

References

Allegrini, J., Dorer, V., Carmeliet, J., 2012a. Influence of the urban microclimate in street canyons on the energy demand for space cooling and heating of buildings. Energ. Buildings 55, 823-832.

Allegrini, J., Dorer, V., Carmeliet, J., 2012b. An adaptive temperature wall function for mixed convective flows at exterior surfaces of buildings in street canyons. Build. Environ. 49, 55-66.

Allegrini, J., Dorer, V., Carmeliet, J., 2015a. Influence of morphologies on the microclimate in urban neighbourhoods. J. Wind En. Ind. Aerod. 144, 108-117.

Allegrini, J., Dorer, V., Carmeliet, J., 2015b. Coupled CFD, radiation and building energy model for studying heat fluxes in an urban environment with generic building configurations. Sustainable Cities and Society 19, 385-394.

Allegrini, J., Carmeliet, J., 2017. Simulations of local heat islands in Zürich with coupled CFD and building energy models. Urban Climate, DOI: 10.1016/j.uclim.2017.02.003.

Arnfield, J, 2003. Two decades of urban climate research: a review of turbulence, exchanges of energy and water, and the urban heat island. Int. J. Climatol. 23, 1-26.

Blocken B, Stathopoulos T, Carmeliet J., 2007. CFD simulation of the atmospheric boundary layer: wall function problems. Atmos. Environ. 41(2): 238-252.

Boppana, V.B.L., Xie, Z.-T., Castro, I.P., 2010. Large-Eddy Simulation of Dispersion from Surface Sources in Arrays of Obstacles. Boundary-Layer Meteorol. 135, 433-454.

Bouyer, J., Inard, C., Musy, M., 2011. Microclimatic coupling as a solution to improve building energy simulation in an urban context, Energ. Buildings 43, 1549-1559.

Bruse, M., Fleer, H., 1998. Simulating surface-plant-air interactions inside urban environments with a three-dimensional numerical model. Environ Modell. Softw. 13, 373-384.

Deng, J., Wong, N.H., Zheng, X., 2016. The Study of the Effects of Building Arrangement on Microclimate and Energy Demand of CBD in Nanjing, China. Proceeding of 4th International Conference on Countermeasures to Urban Heat Island, Singapore.

Fischer, E.M., Schär, C., 2009. Future changes in daily summer temperature variability: driving processes and role for temperature extremes. Clim. Dynm. 33, 917-935.

837 Franke, J., Hellsten, A., Schlünzen, H., Carissimo, B., 2011. The COST 732 best practice guideline
838 for CFD simulation o flows in the urban environment: a summary. Int. J. Environ. Pollut. 44 (1-4),
839 419-427.

840 Gan, Y., Chen, H., 2016. Discussion on the applicability of urban morphology index system for
841 block natural ventilation research. Proceeding of 4th International Conference on Countermeasures
842 to Urban Heat Island, Singapore.

843 Gromke, C.B., Blocken, B., Janssen, W.D., Merema, B., van Hooff, T., Timmermans, H.J.P., 2015.
844 CFD analysis of transpirational cooling by vegetation: Case study for specific meteorological condi-
845 tions during a heat wave in Arnhem, Netherlands. Build. Environ. 83, 11-26.

846 Haldi, F., Robinson, D., 2011. The impact of occupants' behaviour on building energy demand.
847 Journal of Building Performance Simulation 4 (4), 323-338.

848 Hang, J., Yuguo, L., Sandberg, M., Buccolieri, R., Di Sabatino, S., 2012. The influence of building
849 height variability on pollutant dispersion and pedestrian ventilation in idealized high-rise urban are-
850 as. Build. Environ. 56, 346-360.

851 Kämpf, J., 2009. On the modelling and optimisation of urban energy fluxes, PhD thesis n° 4548
852 EPF Lausanne, Lausanne.

853 Launder, B.E., Spalding, D.B., 1974. The numerical computation of turbulent flows. Comput Meth-
854 od Appl M Eng 3, 269-289.

855 Li, D., Bou-Zeid, E., 2013. Synergistic interactions between urban heat islands and heat waves: The
856 impact in cities is larger than the sum of its parts. Journal of Applied Meteorology and Climatology
857 52 (9), 2051-2064.

858 McAdams, W.H., 1954. Heat Transmission, McGraw-Hill Kogakusha, Tokyo.

859 Millward-Hopkins, J.T., Tomlin, A.S., Ma, L., Ingham, D., Pourkashanian, M., 2011. Estimating
860 Aerodynamic Parameters of Urban-Like Surfaces with Heterogeneous Building Heights. Boundary-
861 Layer Meteorol. 141, 443-465.

862 Mirzaei, PA, Haghighat, F., 2010. Approaches to study urban heat island e abilities and limitations.
863 Build. Environ. 45, 2192-201.

864 Moonen, P., Dorer, V., Carmeliet, J., 2011. Evaluation of the ventilation potential of courtyards and
865 urban street canyons using RANS and LES. J. Wind En. Ind. Aerod. 99, 414-423.

866 Moonen, P., Defraeye, T., Dorer, V., Blocken, B., Carmeliet, J., 2012. Urban Physics: Effect of the
867 micro-climate on comfort, health and energy demand. Frontiers of Architectural Research1, 197-
868 228.

869 Nazarian, N., Kleissl, J., 2015. CFD simulation of an idealized urban environment: Thermal effects
870 of geometrical characteristics and surface materials. Urban Climate 12, 141-159.

871 Nazarian, N., Kleissl, J., 2016. Realistic solar heating in urban areas: Air exchange and street-
872 canyon ventilation. Building and Environment 95, 75-93.

873 Oke, T.R., 1987. Boundary Layer Climates, second ed. Methuen, London.

874 Perez, R., Seals, R., Michalsky, J., 1993. All-weather model for sky luminance distribution -
875 preliminary configuration and validation. Sol. Energy 50 (3), 235–243.

876 Pillai, S.S., Yoshie, R., Chung, J., 2010. Experimental and computational studies on heat transfer
877 from urban canopy and its dependence on urban parameters. Proceeding of The Fifth International
878 Symposium on Computational Wind Engineering, Chapel Hill, USA.

879 Pillai, S.S., Yoshie, R., 2015. Simulation of heat transfer from canopy surfaces using low-Reynolds
880 number k-e model. Journal of Urban and Environmental Engineering 8 (2), 186-191.

881 Ramponi, R., Blocken, B., de Coo, L.B., Janssen, W.D., 2015. CFD simulation of outdoor ventila-
882 tion of generic urban configurations with different urban densities and equal and unequal street
883 widths. Build. Environ. 92, 152-166.

884 Richards, P.J., Hoxey, R.P., 1993. Appropriate boundary conditions for computational wind engi-
885 neering models using the k-ε turbulence model. J. Wind En. Ind. Aerod. 46-47, 145-153.

886 Robine, J.-M., Cheung, S. L. K., Le Roy, S., Van Oyen, H., Griffiths, C., Michel, J.-P., Herrmann,
887 F. R., 2008. Death toll exceeded 70,000 in Europe during the summer of 2003. Comptes Rendus
888 Biologies 331, 171-178.

889 Robinson, D., Stone, A., 2006. Internal illumination prediction based on a simplified radiosity algo-
890 rithm. Sol. Energy 80 (3), 260-267.

891 Robinson, D., 2011. Computer Modelling for Sustainable Urban Design: Physical Principles, Meth-
892 ods and Applications, Earthscan, London.

893 Saneinejad, S., Moonen P., Carmeliet J., 2014. Coupled CFD, radiation and porous media model for
894 evaluating the micro-climate in an urban environment. J. Wind En. Ind. Aerod. 128, 1-11.

895 Santamouris, M., Papanikolaou, N., Livada, I., Koronakis, C., Georgakis, A., 2001. On the impact
896 of urban climate on the energy consumption of buildings. Sol. Energy 70 (3), 201-216.

897 Santiago, J.L., Krayenhoff, E.S., Martilli A., 2015. Flow simulations for simplified urban configura-
898 tions with microscale distributions of surface thermal forcing. Urban Climate 9, 115-133.

899 Schär, C., Vidale, P.L., Lüthi, D., Frei, C., Häberli, C., Liniger, M.A., Appenzeller, C, 2004. The
900 role of increasing temperature variability in European summer heatwaves. Nature 427, 332-336.

901 SIA 2024, 2006. Standard-Nutzungsbedingungen für die Energie- und Gebäudetechnik, SIA, Swiss
902 Association of Engineers and Architects, Zürich.

Tominaga, Y., Mochida, A., Yoshie, R., Kataoka, H., Nozu, T., Yoshikawa, M., Shirasawa, T., 2008. AIJ guidelines for practical applications of CFD to pedestrian wind environment around buildings. J. Wind Eng. Ind. Aerodyn. 96, 1749–1761.

Tominaga, Y., 2012. Visualization of city breathability based on CFD technique: case study for urban blocks in Niigata City. J. Vis. 15, 239-276.

Toparlar, Y., Blocken, B., Vos, P., van Heijst, G.J.F, Janssen, W.D., van Hooff, T., Montazeri, H., Timmermans, H.J.O, 2015. CFD simulation and validation of urban microclimate: A case study for Bergpolder Zuid, Rotterdam. Build. Environ. 83, 79-90.

Van Hooff, T., Blocken, B., 2010. Coupled urban wind flow and indoor natural ventilation modelling on a high-resolution grid: A case study for the Amsterdam ArenA stadium. Environ Modell. Softw. 25, 51-65.

Walter, E., Kämpf , J. H., 2015. A verification of CitySim results using the BESTEST and monitored consumption values. Proceeding of Building Simulation Applications BSA 2015, Bozen-Bolzano, Italy.

Watkins, R., Palmer, J., Kolokotroni, M., Littlefair, P., 2002. The London Heat Island – results from summertime monitoring. Build. Serv. Eng. Res. Technol. 23 (2), 97-106.

Yaghoobian, N., Kleissl, J., U, K.T.P., 2014. An Improved Three-Dimensional Simulation of the Diurnally Varying Street-Canyon Flow. Boundary-Layer Meteorology 153 (2), 251-276.

Zaki, S.A., Hagishima, A., Tanimoto, J., Ikegaya N., 2011. Aerodynamic Parameters of Urban Building Arrays with Random Geometries. Boundary-Layer Meteorol. 138, 99-120.